PMT calibration of a scintillation detector using primary scintillation

Jinst

PUBLISHED BY IOP PUBLISHING FOR SISSA MEDIALAB

RECEIVED: *October 24, 2014*
ACCEPTED: *December 15, 2014*
PUBLISHED: *February 23, 2015*

16th INTERNATIONAL WORKSHOP ON RADIATION IMAGING DETECTORS
22–26 JUNE 2014,
TRIESTE, ITALY

PMT calibration of a scintillation detector using primary scintillation

The NEXT collaboration

E.D.C. Freitas,[a] L.M.P. Fernandes,[a] N. Yahlali,[b] J. Pérez,[m] V. Álvarez,[b] F.I.G. Borges,[a] M. Camargo,[h] S. Cárcel,[b] S. Cebrián,[c] A. Cervera,[b] C.A.N. Conde,[a] T. Dafni,[c] J. Díaz,[b] R. Esteve,[e] P. Ferrario,[b] A.L. Ferreira,[g] V.M. Gehman,[d] A. Goldschmidt,[d] H. Gómez,[c] J.J. Gómez-Cadenas,[b] D. González Díaz,[c] R.M. Gutiérrez,[h] J. Hauptman,[i] J.A. Hernando Morata,[j] D.C. Herrera,[c] I.G. Irastorza,[c] L. Labarga,[k] A. Laing,[b] I. Liubarsky,[b] N. Lopez-March,[b] D. Lorca,[b] M. Losada,[h] G. Luzón,[c] A. Marí,[e] J. Martín-Albo,[b] A. Martínez,[b] G. Martínez Lema,[j] T. Miller,[d] F. Monrabal,[b] M. Monserrate,[b] F.J. Mora,[e] L.M. Moutinho,[g] J. Muñoz Vidal,[b] M. Nebot Guinot,[b] D. Nygren,[d] C.A.B. Oliveira,[d] J. Pérez,[k] J.L. Pérez Aparicio,[l] M. Querol,[b] J. Renner,[d] L. Ripoll,[n] A. Rodríguez,[c] J. Rodríguez,[b] F.P. Santos,[a] J.M.F. Dos Santos,[a,1] L. Seguí,[c] L. Serra,[b] D. Shuman,[d] A. Simón,[b] C. Sofka,[o] M. Sorel,[b] J.F. Toledo,[e] J. Torrent,[n] Z. Tsamalaidze,[f] J.F.C.A. Veloso,[g] J.A. Villar,[c] R. Webb,[o] J. White[o] and C.M.B. Monteiro[a]

[a] *Departamento de Fisica, Universidade de Coimbra , Rua Larga, 3004-516 Coimbra, Portugal*

[b] *Instituto de Física Corpuscular (IFIC), CSIC & Universitat de Valencia, Calle Catedrático José Beltrán, 2, 46980 Paterna, Valencia, Spain*

[c] *Laboratorio de Física Nuclear y Astropartículas, Universidad de Zaragoza, Calle Pedro Cerbuna, 12, 50009 Zaragoza, Spain*

[d] *Lawrence Berkeley National Laboratory (LBNL), Cyclotron Road, Berkeley, California 94720, U.S.A.*

[e] *Instituto de Instrumentación para la Imagen Molecular (I3M), Universitat Politècnica de València, Camino de Vera, s/n, Edificio 8B, 46022 Valencia, Spain*

[1] Corresponding author.

doi:10.1088/1748-0221/10/02/C02039

2015 JINST 10 C02039

[f] *Joint Institute for Nuclear Research (JINR), Joliot-Curie, 6, 141980 Dubna, Russia*
[g] *Institute of Nanostructures, Nanomodelling and Nanofabrication (I3N), Universidade de Aveiro, Campus de Santiago, 3810-193 Aveiro, Portugal*
[h] *Universidad Antonio Nariño, Centro de Investigaciones, Carretera 3 Este, 47A-15, Bogotá, Colombia*
[i] *Department of Physics and Astronomy, Iowa State University, 12 Physics Hall, Ames, Iowa 50011-3160, U.S.A.*
[j] *Instituto Gallego de Física de Altas Energías, Universidad de Santiago de Compostela, Campus Sur, Rua Xosé María Suárez Nuñez, s/n, 15782 Santiago de Compostela, Spain*
[k] *Departamento de Física Teórica, Universidad Autónoma de Madrid, Campus de Cantoblanco, 28049 Madrid, Spain*
[l] *Departamento de Mecánica de Medios Continuos y Teoría de Estructuras, Universitat Politècnica de València, Camino de Vera, s/n, 46071 Valencia, Spain*
[m] *Instituto de Física Teórica (IFT), CSIC & Universidad Autónoma de Madrid, Campus de Cantoblanco, 28049 Madrid, Spain*
[n] *Escola Politècnica Superior, Universitat de Girona, Av. Montilivi, s/n, 17071 Girona, Spain*
[o] *Department of Physics and Astronomy, Texas A&M University, College Station, Texas 77843-4242, U.S.A.*

E-mail: jmf@gian.fis.uc.pt

ABSTRACT: We have studied the calibration of PMTs in scintillation detectors, inducing single electron response on the PMT from primary scintillation produced by x-ray interaction. The results agree with those obtained by the commonly used single electron response (SER) method, which uses LED light pulses to induce the PMT SER. The use of the primary scintillation for PMT calibration will be convenient in situations where the PMT is already in situ, when it becomes difficult or even impossible to apply the SER method, e.g. in commercial sealed scintillator/PMT devices. Furthermore, we have experimentally investigated the possibility of fitting the high-charge tail of the PMT SER pulse-height distribution to an exponential function, inferring the PMT gain from the inverse of the exponent. The results of the exponential fit method agree with those obtained by the SER method for pulse-height distributions resulting from an average number of around 1.0 photoelectrons reaching the first dynode per light/scintillation pulse. The SER method has higher precision and, therefore, is used in a larger number of applications. Nevertheless, the exponential fit method will be useful in situations where the single photoelectron peak is under the background or noise peak and it may present an alternative, simple way, for relative gain calibration of PMT arrays as well as for monitoring the PMT gain variations.

KEYWORDS: Photon detectors for UV, visible and IR photons (vacuum) (photomultipliers, HPDs, others); Scintillators, scintillation and light emission processes (solid, gas and liquid scintillators)

2015 JINST 10 C02039

Contents

1 Introduction 1

2 Experimental setup and method 2

3 Experimental results and discussion 4

4 Conclusions 7

1 Introduction

The knowledge of the PMT gain can be important in many different situations. PMTs are widely used as photosensors of scintillation detectors, which are extensively applied to x-ray spectrometry, particle detection for high-energy physics and rare event detection. The knowledge of the PMT gain allows the determination of the number of photoelectrons released by the photocathode, following the measurement of the total number of electrons collected in the anode. The determination of this number is an important parameter for the studies of the scintillator response to photons and charged particles and the respective dependence on energy. In particular, the absolute energy dissipated in the scintillators is related to the number of photons produced which, in turn, is related to the number of photoelectrons emitted by the PMT photocathode.

An effective standard method for PMT gain determination is achieved by obtaining the PMT response to single photoelectron (SER) [1–3]. Usually, a LED is used to illuminate the PMT at very low light intensity in order to induce single photoelectron response of the PMT. The position of the charge peak produced by single photoelectron emission is measured relative to the position of the pedestal peak (the electronic noise peak, which corresponds to zero induced photoelectrons). If the amount of light is small enough, the single photoelectron emission is dominant over multiple photoelectron emission cases. Upon illumination of the PMT photocathode, the peak distribution associated with events resulting from a given number of photoelectrons reaching the first dynode, can be approximated to a Gaussian and the relative position of the centroid of this Gaussian is proportional to the number of photoelectrons hitting the first dynode, while the value of the Gaussian area, which is related to the probability of occurrence of the corresponding event, obeys a Poisson distribution [1–3]. Therefore, either the SER is deconvoluted in order to determine the position of the peak corresponding to events with single photoelectron emission, or the amount of LED light hitting the PMT is reduced to a point where the probability of having multiple photoelectron emission is less than a few percent, when compared to the probability for single photoelectron emission. In this case, the photoelectron peak in the charge spectrum is well described by a single Gaussian function. In many experiments, the PMT gain is measured before assembling (e.g. see [4]) or even by placing one or more LEDs and/or optical fibres inside the detector, in order to allow the monitoring of the PMT gain in situ (e.g. see [5]). However, there are many cases where the scintillator

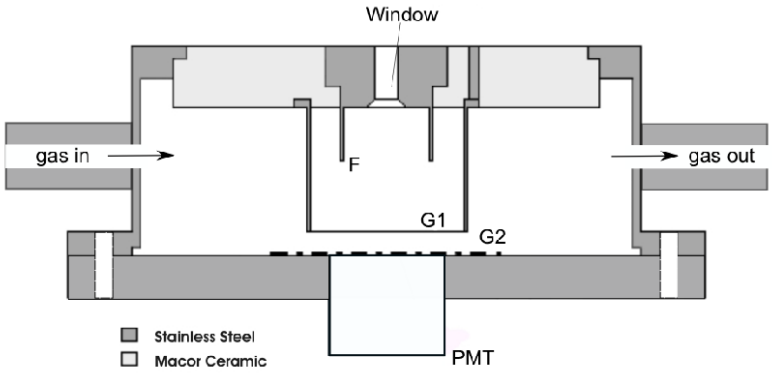

Figure 1. Schematic of the xenon GPSC used in this work.

and the PMT are sealed together being inaccessible to LED light, e.g. as is the case in commercial scintillation detectors, where the above method cannot be used.

In this work, we have investigated the possibility of calibrating a PMT of a scintillation detector using the primary scintillation produced by the interaction of radiation. We used xenon as the scintillator in a Gas Proportional Scintillation Counter (GPSC) [6]. The detector electronic noise was low enough to be able to get the PMT single photoelectron (SPE) peak out of the noise pedestal. Nevertheless, we show that it is possible to monitor the PMT gain in the case when the background noise obscures the SPE peak, making use of the high-charge tail resulting from the multiple photoelectron emission produced by the primary scintillation. An exponential function is fitted to this tail, being the PMT average gain extracted from the inverse of the exponent of this fit. The approximation of the PMT single electron response to an exponential-like distribution has already been described in the literature [7–11].

2 Experimental setup and method

The GPSC used in this work was built to study the performance of an Hamamatsu R8520-06SEL photomultiplier for detecting primary and secondary (electroluminescence) scintillation produced as a result of x-ray absorption in xenon, at room temperature [12]. The schematic of the GPSC is presented in figure 1 and was described in detail in [12].

The GPSC body is made of stainless steel. The R8520-06SEL PMT was glued with low vapour pressure epoxy (TRA-CON 2116) to the anode plane, the bottom base of the GPSC body, as shown in figure 1. The GPSC upper part is a Macor disk with aluminized Kapton x-ray window and focusing electrode F insulated from the detector body. The Macor is glued using the same epoxy already mentioned above. The bottom base is vacuum sealed to the GPSC upper part by compressing an indium gasket in between. The drift/conversion region is 3 cm long and is located between window and mesh G1, while the electroluminescence gap, 0.5 cm thick, is located between mesh G1 and the anode plane (mesh G2), placed on top of the PMT quartz window. G1 holder is a stainless steel cylinder perforated with holes to allow gas circulation.

A ^{55}Fe source is positioned outside the chamber, on top of the detector window and inside a 1-mm in diameter lead collimator. A thin chromium film is placed between the radioactive source

2015 JINST 10 C02039

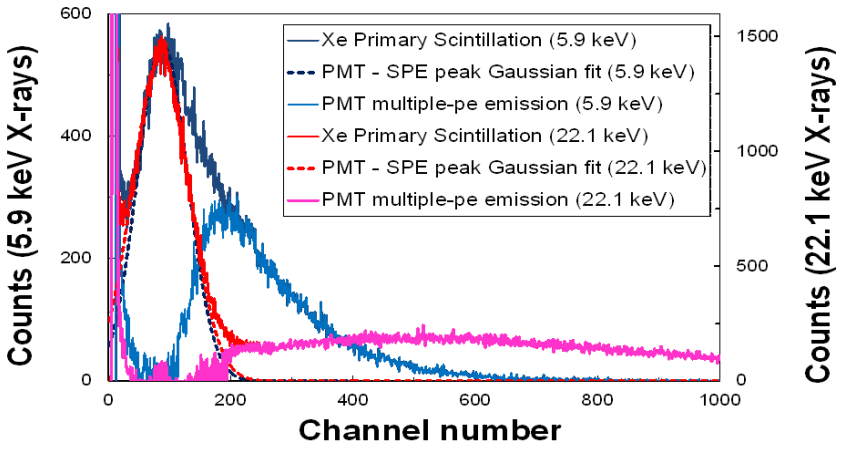

Figure 2. Pulse-height distributions obtained in the detector, with no electric fields applied to either drift and scintillation region and for a PMT bias voltage of 730 V, for 5.9 keV X-rays from a ^{55}Fe radioactive source and for x-rays emitted from a ^{109}Cd radioactive source.

and the collimator to efficiently reduce the interaction of 6.4 keV x-rays (Mn K_β line) in the gas volume. After the absorption of the x-ray by a xenon atom, primary scintillation is produced as a result of collisional processes involving the photoelectron and other Auger and shake-off electrons with the gas atoms. The amplitude of the primary scintillation pulses is very low and difficult to distinguish from the noise or background pulses [12].

In a former study [12], we have shown that the primary scintillation is independent of the electric field applied to the conversion region and independent of the xenon pressure. In addition, we have measured the xenon primary scintillation yield and the average number of primary scintillation photons hitting the PMT active area per 5.9 keV X-ray absorption. On average, 81 vacuum ultraviolet (VUV) scintillation photons, ∼172 nm, are produced per 5.9 keV X-ray absorption in xenon and only 2 of them, on average, reach the PMT active area, in our setup [12]. Since the quantum efficiency of the used PMT is about 33% for xenon VUV (QE enhanced, relative to the standard Hamamatsu R8520 PMT series), 5.9 keV x-ray interactios in our detector leads to a pulse-height distribution resulting from either single-photoelectron and multiple-photoelectron response of the PMT, with an average number of 0.7 pe/scintillation pulse.

Figure 2 shows the pulse-height distribution recorded with the MCA for the primary scintillation resulting from 5.9 keV and 22 keV x-ray interactions in xenon, with no electric fields applied to the GPSC drift and scintillation regions. In order to access the contribution of background pulses resulting from the PMT dark current and/or from residual visible light entering the chamber, energy spectra with and without x-ray irradiation were recorded. In this way, the pulse-height distribution for that background could be identified and subtracted from the raw spectra. The count rate of this background decreases by improving the light shielding of the detector.

As shown, similar distributions were obtained in the low-amplitude region for both cases, while the broader pulse-height distribution extending towards the high-amplitude region depends on the x-ray energy. The low-amplitude peak results from single-photoelectron (SPE) emission from the PMT photocathode, due to the x-ray induced primary scintillation and to other low scintillation processes with even lower photon number, e.g. luminescence and/or fluorescence of the

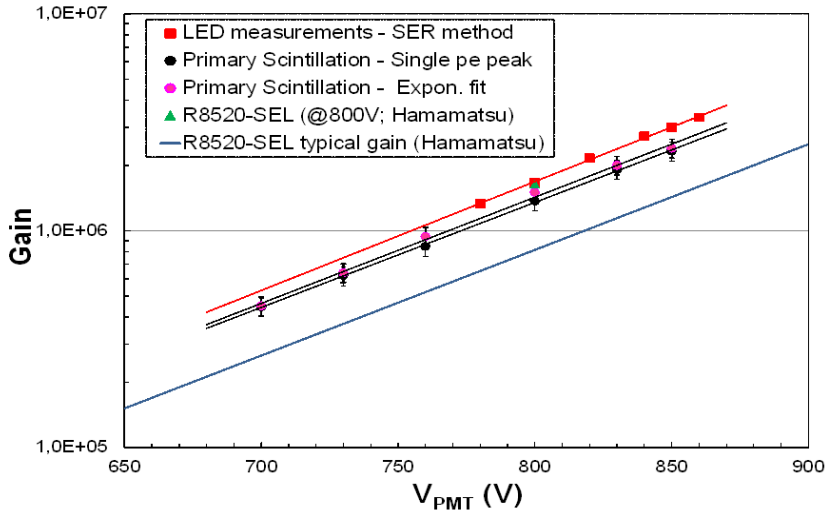

Figure 3. PMT Gain as a function of the biasing voltage: (grey circles) as obtained from the SPE peak position resulting from the primary scintillation pulses produced by radiation interaction in the detector; (diamonds) as obtained from the SER method, using LED light pulses to induce 0.08 pe/light pulse; (pink circles) as obtained from the exponential fit to the pulse-height distributions resulting from the multiple-photoelectron emission by the PMT photocathode as a consequence of the detection of primary scintillation; (triangle) value obtained by Hamamatsu at 800V; and (blue line) typical gain curve for the standard (not QE enhanced) R8520 PMT, provided by Hamamatsu [13].

detector materials induced by the presence of x-ray and/or VUV photon interaction. The distribution due to multiple-electron emission extends towards the higher amplitude region. Assuming a Gaussian shape for the SPE peak, we can subtract it from the overall pulse-height distribution, obtaining the pulse-height distribution resulting from multiple-photoelectron emission, as shown in figure 2.

The MCA channel number was calibrated in terms of number of electrons by means of a precise pulse generator and a known capacitance coupled to the preamplifier input. Thus, the position of the SPE peak in number of electrons directly gives the PMT average gain, being the pedestal of our electronic chain within one channel away from channel number 0.

3 Experimental results and discussion

The experimental results obtained for the PMT gain using the SPE peak position are shown in figure 3. The PMT gains obtained using the standard SER technique are also shown in figure 3, together with the value measured by Hamamatsu at 800V and supplied in the PMT datasheet. In figure 3 we also plot the typical gain for the standard R8520 PMT series [13].

The measurements for the SER method, with the LED, were performed in a standard setup [1–3], placing the PMT in a black-box, after the GPSC disassembling. Gains could not be measured with the SER method for PMT voltages below 780 V, because the single-photoelectron peak of the pulse-height distribution gets under the electronic noise (pedestal). On the other hand, in our scintillation detector we could measure gains for PMT voltages lower than 700V. The results obtained

using the primary scintillation agrees with those obtained using the SER method, within 15%. However, a systematic deviation towards lower gain values is observed. This systematic error may have arisen from the charge calibration of the GPSC electronic chain, e.g. from the nominal value of the capacitor.

The typical PMT gain value provided by Hamamatsu at 800 V was measured taking the ratio of anode and photocathode currents, being the product of the interstage gains in the dynode chain and the collection efficiency of the photoelectrons at the first dynode [13]. This collection efficiency, which is typically between 80 and 100%, is not included in the average gain provided by the SER and scintillation methods since we measure the effective charge gain through the dynode chain. Therefore, the SER value is in agreement with that of Hamamatsu.

In addition to the above studies, we investigated the possibility of accessing the PMT gain using an exponential fit to the high-amplitude tail of the pulse-height distribution of the primary scintillation from 5.9 keV interactions in our detector. The approximation of the PMT response to an exponential-like distribution has already been performed in the literature [7–11]. In cases when SPE is overlapped by the noise background peak, it is not possible to determine the PMT gain using the SER or the primary scintillation methods described above. Only the tail in the high-charge side of the distribution is not contaminated by this background.

Figure 4 shows the pulse-height distribution resulting from the primary scintillation of 5.9 keV x-ray interactions after the subtraction of the SPE, for different PMT biasing voltages. Therefore, these distributions include the contribution of PMT pulses due to the multi-photoelectron emission from the photocathode. We have fitted the tails of these distributions to exponential functions of the type:

$$P(q) = ae^{-\frac{q}{q_{\text{avg}}}}, \tag{3.1}$$

being q the charge collected at the PMT anode and q_{avg} the average charge obtained from all the primary scintillation events. If this empirical approximation holds, it is possible to extract the PMT average gain from the exponential fit, given by q_{avg}.

Figure 4 shows that all the tails are very well described by an exponential function and, as the PMT voltage increases, the distributions have a smaller slope and extend to higher amplitudes. The average gains that could be inferred from these slopes, using eq. (3.1), are also plotted in figure 3. As shown in figure 3, the PMT gains obtained by the exponential fit are similar, within errors, to those obtained from the centroid position of the respective SPE peak.

The exponential absorption of the x-rays in xenon may contribute to the high-amplitude tail of the detector response, due to increase in the solid angle subtended by the PMT photocathode relative to the point where the primary scintillation is produced, as the x-ray photon is absorbed deeper in the xenon volume. In the present detector, filled with xenon at 2 bar, the total solid angle variation was 15% for 90% absorption of a 5.9 keV x-ray beam, and the detector response for the primary scintillation resulting from a 5.9 keV x-ray beam is similar for 1, 2 and 3 bar of xenon, as found in [12]. Therefore, the impact of such an effect on the high-amplitude tail of this detector response is negligible compared to that resulting from the PMT response to the primary scintillation, figure 4.

To have a deeper insight of the empirical approximation we made for extracting the PMT gain from the exponential fit, we investigated the PMT pulse-height distribution profiles obtained in the

2015 JINST 10 C02039

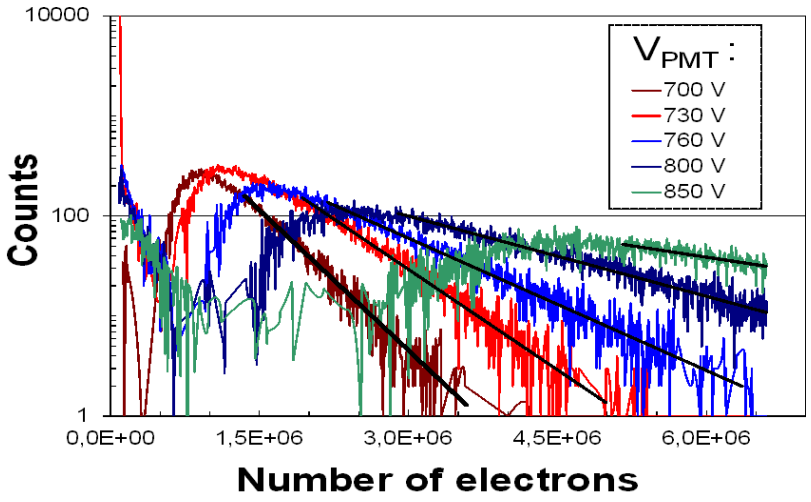

Figure 4. Pulse height distribution of the PMT multiple-photoelectron emission due to xenon primary scintillation resulting from 5.9 keV x-ray absorption for different PMT biasing voltages. These distributions are obtained by subtraction of the SPE peak, fitted by a Gaussian curve. The solid lines represent the exponential fits to the tails.

SER method. While in the primary scintillation measurements the amount of light hitting the PMT active area corresponds to a photocathode average emission of ∼0.7 photoelectrons per scintillation pulse, this number is usually set below 0.1 for the LED light irradiation technique (SER method), in order to reduce the contribution of multiple photoelectron emission by the PMT photocathode to a negligible level. Therefore, to understand the effect of the amount of light detected by the PMT on the determination of the centroid of the SPE peak in the SER method, we have measured this peak position versus the PMT biasing voltage for different levels of light emitted by the LED. The corresponding average photoelectron emission per light pulse varied between 0.30 and 1.38. As expected, the relative position of the SPE peak and, thus, the gain obtained by the SER method does not depend on the LED light level, within the studied range.

After this study, we have applied the exponential fit method to the pulse-height distributions obtained with LED irradiation for different PMT voltages and for different LED light levels. Figure 5a shows typical pulse-height distributions obtained for different PMT voltages and for a LED illumination level corresponding to an average of 0.30 photoelectrons emitted by the photocathode per light pulse. Figure 5b shows typical pulse-height distributions obtained for different LED illumination levels and for a PMT voltage of 800 V.

Figure 6 shows the PMT average gain inferred through the exponential fit to the high-charge tails of the respective SER pulse-height distributions as a function of PMT bias voltage, for different LED light illumination levels. For comparison, The PMT average gain obtained using the SER method, as well as the average gain obtained through the pulse-height distributions of the xenon primary scintillation induced by 5.9 keV x-rays, are also shown. As seen, the PMT gain inferred from the exponential fit method depends on the illumination level of the PMT, i.e. on the amount of light hitting the photocathode. Nevertheless, relative to the gain obtained by measuring the SPE peak position, the attained gains are within 20% for light levels in a range corresponding to an average of 0.7–1.4 photoelectrons amplified in the PMT dynode chain, per light pulse. The

2015 JINST 10 C02039

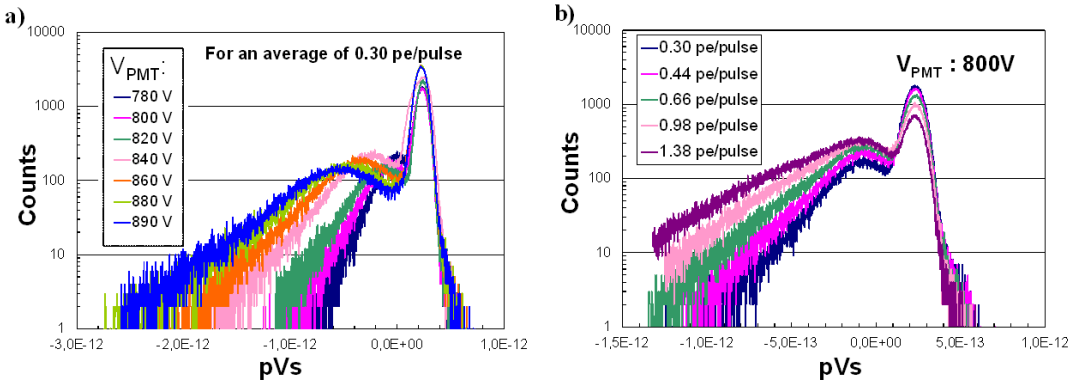

Figure 5. SER PMT pulse height distributions: (a) for constant LED illumination level corresponding to an average of 0.30 photoelectrons emitted by the photocathode per light pulse and different PMT biasing voltages; (b) for a constant PMT biasing voltage of 800 V and different LED illumination levels.

variation of the fitted-exponential gain with the light illumination level indicates that this is not a real gain. The numerical match between the gain obtained through the SPE peak position and that inferred by the fitted exponential slope parameter, under certain illumination conditions, may be a coincidence for the combination of the pulse amplitude and width and the Poisson distributed numbers of photoelectrons, which can be utilized to infer the gain.

For low light illumination, e.g. below an average of 0.1 photoelectrons collected in the first dynode per light pulse, the SER pulse-height distribution of the PMT is well described by a Gaussian function [1–3]. As the amount of light illuminating the PMT increases, the probability for multiple-photoelectron emission also increases and the pulse-height distribution consists of a sum of the different Gaussians corresponding to events with different numbers of photoelectrons hitting the first dynode. The position of the centroid of each Gaussian presents a linear increase with the number of photoelectrons hitting the first dynode, while the value of the Gaussian area, which is related to the probability of occurrence of the corresponding event, obeys a Poisson distribution [1, 2]. Therefore, the sum of these multiple Gaussians leads to a pulse-height distribution with a high-amplitude tail that can be approximated to an exponential function. The gain extracted from the proposed method is more accurate for an average emission of about 1 photoelectron per light pulse, as shown in figure 6. More work needs to be performed, e.g. developing a mathematical model, according to the conditions described above, to show the match between the obtained slope parameter and the SPE relative peak position.

The proposed method for obtaining the gain by applying the exponential fit to the high amplitude tails of pulse-height distributions resulting from primary scintillation events has been applied successfully by the NEXT Collaboration [14] to monitor the gain variations of the PMTs used in the NEXT-DEMO TPC [15, 16]. The reference gains in NEXT-DEMO are obtained using the SER method, but the evolution of gain with time is monitored using the method described in this paper.

4 Conclusions

We have measured the average gain of a PMT assembled inside a GPSC by collecting the pulse height distributions from the primary scintillation produced in xenon by the interaction of 5.9 keV x-rays. These primary scintillation pulses induce, on average, about 0.7 photoelectrons collected

2015 JINST 10 C02039

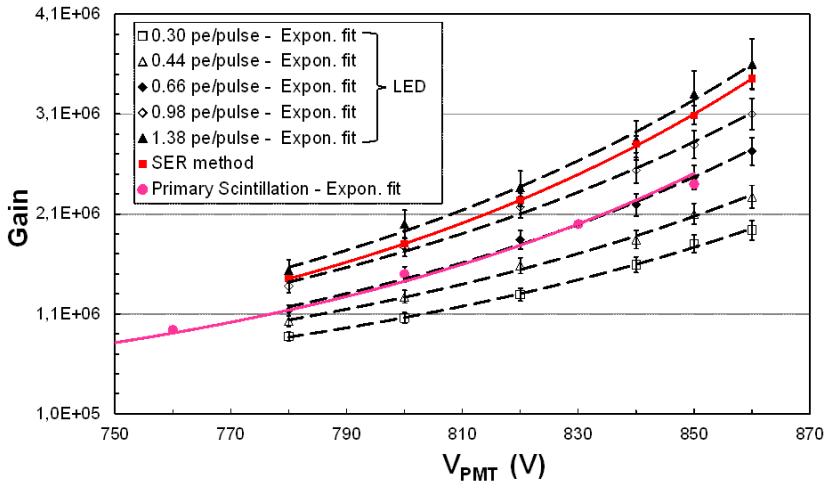

Figure 6. PMT average gain as a function of biasing voltage, obtained with exponential fits to the tails of the pulse-height distributions resulting from different average numbers of photoelectrons emitted by the photocathode per light pulse. The PMT average gain obtained from the pulse-height distributions of xenon primary scintillation, as well as that obtained through the SER single photoelectron peak position determination, are also presented.

in the PMT dynode chain. We found that the high-amplitude tails of these pulse height distributions are well described by an exponential function, being possible to infer the PMT average gain from the inverse of the exponent. The results obtained with this method are consistent with those obtained through the single-photoelectron peak position.

The present studies have shown that PMT gain calibration, obtained from the fit of an exponential function to the high-charge tail of the PMT pulse-height distributions, obtained with the SER method, is a valid procedure for PMT illumination within suitable levels, inducing on average around 1 photoelectron per scintillation pulse. Lower scintillation levels will lead to inferred lower gain values, when comparing to those obtained with the single-photoelectron peak position. Nevertheless, the inferred gain is still within 20% of the true gain for scintillation levels inducing on average 0.7 to 1.4 photoelectrons per scintillation pulse.

This method, although not as precise as the SER one, can be useful when the PMT is sealed together with the scintillator, like in many commercial scintillation counters, rendering the use of LEDs impossible. In addition, it can be used even when the detector background noise is high, covering the single-photoelectron peak, since only the high-charge tail is needed. This method may also present an expedite alternative way to perform relative gain calibrations in PMT arrays and/or monitor PMT gain variations.

Future work will investigate the possibility to obtain a mathematical model that can show the relation between the SPE peak position and the slope of the exponential fit to the high-charge tail of the SER pulse-height distribution.

Acknowledgments

The NEXT experiment is supported by the following agencies and institutions: the European Research Funding through an ERC Advanced Grant (NEXT 2013); Ministerio de Economía

y Competitividad of Spain under grants CONSOLIDER-Ingenio 2010 CSD2008- 0037 (CUP), FPA2009-13697-C04-04 and FIS2012-37947-C04; the Portuguese FCT and FEDER through program COMPETE, project PTDC/FIS/103860/2008. C.M.B. Monteiro acknowledges grant SFRH/BPD/76842/2011 from FCT.

References

[1] E.H. Bellamy et al., *Absolute calibration and monitoring of a spectrometric channel using a photomultiplier*, *Nucl. Instrum. Meth.* **A 339** (1994) 468.

[2] R. Dossi et al., *Methods for precise photoelectron counting with photomultipliers*, *Nucl. Instrum. Meth.* **A 451** (2000) 623.

[3] I. Chirikov-Zorin et al., *Method for precise analysis of the metal package photomultiplier single photoelectron spectra*, *Nucl. Instrum. Meth.* **A 456** (2001) 310.

[4] A. Bueno et al., *Characterization of large area photomultipliers and its application to dark matter search with noble liquid detectors*, 2008 *JINST* **3** P01006.

[5] XENON100 collaboration, E. Aprile et al., *The XENON100 dark matter experiment*, *Astropart. Phys.* **35** (2012) 573 [arXiv:1107.2155].

[6] J.M.F. dos Santos et al., *Development of portable gas proportional scintillation counters for X-ray spectrometry*, *X-Ray Spectrom.* **30** (2001) 373.

[7] G.F. Knoll, *Radiation detection and measurements*, 4th edition, Wiley, New York U.S.A. (2010).

[8] J.R. Prescott, *A statistical model for photomultipliers single-electron statistics*, *Nucl. Instrum. Meth.* **A 39** (1966) 173.

[9] F.W. Inman and J.J. Muray, *Variations in single photon pulse height distribution with focusing voltage in photomultipliers*, *IEEE Trans. Nucl. Sci.* **16** (1969) 62.

[10] A. Leisos, S.E. Tzamarias and A. Tsirigotis, *Performance of the NESTOR calibration system*, NESTOR Internal Report HOU-NS-TR-2004-02-EN (2004).

[11] A.G. Tsirigotis, *NESTOR first results*, *Eur. Phys. J.* **C 33** (2004) S956.

[12] L.M.P. Fernandes et al., *Primary and secondary scintillation measurements in a Xenon gas proportional scintillation counter*, 2010 *JINST* **5** P09006.

[13] Hammatsu Photonics K.K., *Electron tube division, photomultipiers tubes: basics & applications — Hamamatsu photonics*, www.hamamatsu.com.

[14] V. Álvarez et al., *NEXT-100 technical design report: executive summary*, 2012 *JINST* **7** T06001.

[15] V. Álvarez et al., *Initial results of NEXT-DEMO, a large-scale prototype of the NEXT-100 experiment*, 2013 *JINST* **8** P04002.

[16] V. Álvarez et al., *Operation and first results of the NEXT-DEMO prototype using a silicon photomultiplier tracking array*, 2013 *JINST* **8** P09011.

2015 JINST 10 C02039